Modeling sorghum-cowpea intercropping for a site in the savannah zone of Mali: Strengths and weaknesses of the Stics model

Amadou Traoré, Gatien Falconnier, Alassane Ba, Fagaye Sissoko, Benjamin Sultan, François Affholder

Modelling sorghum-cowpea intercropping in semi-arid sub-Saharan Africa: strengths and weaknesses of the Stics model

Amadou Traoré[1], Gatien N. Falconnier[2,3], Alassane Ba[1], Fagaye Sissoko[1], Benjamin Sultan[4], François Affholder[2,3]

Corresponding author : Gatien.falconnier@cirad.fr
[1]IER (Institut d'Economie Rurale, Mali)
[2]AIDA, Univ Montpellier, CIRAD, Montpellier, France
[3]CIRAD, UPR AIDA, F-34398 Montpellier, France
[4]ESPACE-DEV, Univ Montpellier, IRD, Univ Guyane, Univ Réunion, Univ Antilles, Univ Avignon

Abstract:

Intercropping is a key entry point for sustainable intensification of cropping systems in sub-Saharan Africa where variable rainfall conditions prevail. Crop simulation models can complement field experiments to assess the agronomic and environmental performances of intercropping systems under diverse climatic conditions, including hypothetical future climate. So far, crop models that can handle intercropping, such as STICS, have not often been extensively evaluated for tropical conditions and for species grown by farmers in sub-Saharan Africa. The objective of this study was to evaluate the performance of the calibrated STICS model to simulate sorghum-cowpea intercropping systems in rainfed conditions in West Africa. We used data from field experiments conducted at the N'Tarla Agronomic Station in Mali in 2017 and 2018. Two varieties of sorghum (local and improved) with contrasting photoperiod sensitivities were grown as sole crop and intercropped with cowpea, with additive design. Two sowing dates and two levels of mineral fertilization were also investigated. Model simulations were evaluated with observed data for phenology, leaf area index (LAI), aboveground biomass, grain yield and in-season soil moisture. Large variations in aboveground biomass of sorghum and cowpea was observed in the experiment (i.e. 3.5 – 9.6 t/ha for sorghum and 0.4 - 2.5 t/ha for cowpea), owing to the treatments (i.e. sole vs intercrop, early vs late sowing, no fertiliser input vs fertiliser input). Such variations were satisfactorily reproduced by the model, with EF of 0.81 in

calibration and 0.58 in evaluation (with relative RMSE of 23 and 43%). The two main observed features of the intercropping system was well reproduced by the model. Firstly, cowpea and sorghum aboveground biomass decreased with intercropping compared with sole cropping, and the decrease in cowpea biomass was greater than the decrease in sorghum biomass. Secondly, despite a reduction in sorghum and cowpea yield, Land Equivalent Ratio of the intercropping for aboveground biomass was always above one. With regard to grain yield, observed LER was above one only in the non-fertilised treatment. The model failed at reproducing this behaviour, probably because of insufficiently accurate calibration of the process leading to grain yield formation: rRMSE for grain yield was 49% in calibration and 41% in evaluation. Based on these findings, we discuss avenues to improve model calibration and use the model to explore options for sustainable intensification in land constrained sub-Saharan Africa.

Keywords: Competition, sowing date, varieties, fertilization, contrasting seasons, aboveground biomass, Mali

I. Introduction

Rainfed agriculture is the most important sector for food security in sub-Saharan Africa (Gowing and Palmer, 2008). However, the region is characterized by low yield due to limited nutrients inputs and weed pressure (Affholder et al., 2013). Rural farmers do not have access to inputs, and low levels of investment in infrastructure generates high transaction costs that lowers the profitability of agricultural activities. These constraints will likely be exacerbated by climate change: the frequency and severity of extreme weather events such as drought and floods is predicted to increase (Connolly-Boutin and Smit, 2015; Diedhiou et al., 2018; Sultan and Gaetani, 2016).

West Africa must produce more to feed a rapidly growing population. Sorghum is one of the main food crops in West Africa. Sorghum yield is expected to decrease by 13% due to climate change (Sultan et al., 2014). Improving soil fertility and agricultural productivity while adapting to climate change have

53 therefore become the priority objectives of agricultural policies in West African countries
54 (CORAF/WECARD, 2008). In land constrained areas with limited availability of arable land and
55 pastures, intensification of agro-systems will be key. But the experience gained in developed countries
56 indicates that excessive artificialization of the environment, as in “conventional” intensification of
57 agriculture, causes environmental damages. A new form of agriculture to increase agricultural
58 productivity while preserving the ecosystem services that ensure long-term environmental sustainability
59 is needed. At cropping system level, the concept of ecological intensification was coined by to define the
60 set of principles and means necessary to increase primary productivity in the world's major cereal agro-
61 ecosystems (Cassman, 1999). Productivity increase can be achieved by capitalizing on the ecological
62 processes in agro-ecosystems (e.g. biological N_2 fixation), aiming at reducing the use of and need for
63 external inputs (Tittonell and Giller , 2013). Innovative cropping systems for ecological intensification
64 need to be assessed with meaningful agronomic, environmental and economic indicators (Affholder et
65 al., 2014). Key ecological services such as carbon storage and biological diversity also need to be
66 addressed (Bonny , 2011).
67 Legumes offer good prospects to increase yield in line with the principles of ecological intensification:
68 legumes can improve soil fertility (Gbakatchetche et al.,2010), and provide crucial nutrients carry-overs
69 for the subsequent cereal crop (Carsky et al., 2003). Intercropping is the cultivation of two or more
70 species or varieties at the same spatial and temporal resolution (Andrews and Kassam, 1976). In
71 cereal-legume intercropping, inter-species complementarity and facilitation processes can lead to a
72 production benefit of intercropping compared with sole cropping (Li et al., 2003, 1999; Vandermeer,
73 1989). Water use efficiency is greater in intercropping than in sole cropping (Tsubo et al., 2004, Balde et
74 al., 2011). However, the expected benefits of intercropping cereals with legumes are not always
75 obtained in the context of sub-Saharan Africa due to constraints related to cultivar, sowing dates and
76 fertilization levels. Intercropping benefits may be jeopardized by competitions for light, nutrients or water
77 between the intercropped species (e.g. Baldé et al., (2011)). Shifts from competition to facilitation will

depend on climate, soils and crop management (Cooper et al., 2008). Appropriate and site-specific recommendations for intercropping management requires replicated experiments across contrasting sites. In order to account for climate inter-annual variations, the experiments would need to run over several years, which is challenging in terms of time, cost and technical expertise (Knörzer et al., 2011). To address such limitations, crop simulation models have been used to assess the agronomic and environmental performances of cropping systems under diverse climatic conditions, including hypothetical future climate (Boote et al., 1996). Crop models able to deal with intercropping systems are scant. So far, few studies have been conducted on cereal-legume intercropping. Chimonyo et al. (2016) evaluated the ability of the calibrated APSIM model (The Agricultural Production Systems sIMulator) to reproduce sorghum-cowpea intercropping productivity and water use efficiency in potential (i.e. fully irrigated) and water-stressed (i.e. rainfed) conditions, in South Africa. Despite overall promising simulation accuracy for partitioning of solar radiation between the dominant (sorghum) and understory crop (cowpea), the authors showed that water use efficiency of the intercrop was overestimated by the model in rainfed conditions, probably because of an inadequate simulation of water stress. The latter could be improved with soil calibration based on in-season water measurements. The experiment was set with adequate N fertilizer inputs, so that intercrop response to varying N input was not investigated. Masvaya (2019) also investigated the accuracy of APSIM model in simulating sorghum-cowpea intercropping performance in semi-arid zone in Zimbabwe. The model accurately reproduced grain yield of the two crops for contrasting seasons, soils and nitrogen inputs. However, the model could not be evaluated for intermediary variables (e.g. LAI, soil water), leaving the risk of compensation errors. The STICS model (multidisciplinary simulator for standard crops) was calibrated for wheat-pea intercrop (Corre-Hellou et al., 2009). The model successfully simulated the interactions between the intercropped species for nitrogen uptake but failed to accurately reproduce competition for light. So far, the STICS model has not been tested for intercrops of very contrasting height, as it is the case of sorghum and cowpea for example.

This study focuses on sorghum-cowpea intercropping. The objective was to calibrate and evaluate the ability of the STICS soil-crop model to (i) simulate the growth and productivity of a sorghum-cowpea intercropping, (ii) account for possible species competition and/or facilitation for the use of light, water and nitrogen and (iii) test its ability to reproduce the impact of contrasting sorghum varieties, sowing date and fertilization on aboveground biomass and grain yield. Data from two years (2017, 2018) from an experiment conducted at the N'Tarla Agronomic Research Station in Mali were used.

II. MATERIAL AND METHOD

2.1 Study Area

This research was conducted at N'Tarla research station (12.6193°N, -5.689°W) in southern Mali. The climate is typical of the semi-arid Sudano-Sahelian zone of West Africa. The rainy season starts in May and ends in October. Average annual rainfall varies between 800 and 1000 mm. Seasonal average temperature is 29 ◦C (Traore et al., 2013). Farming systems are mixed agro-sylvo-pastoral systems. Cotton (Gossypium hirsutum L.) is the main cash crop and is grown in rotation with sorghum (*Sorghum bicolor (L) Moench*), millet (Pennisetum glaucum (L.) R.Br.), maize (*Zea mays L.*) and legumes such as groundnut (*Arachis hypogaea L.*) and cowpea (*Vigna unguiculata (L) Walp.*). Mineral fertilizer are applied on cotton and maize, with nutrient carry-over benefitting the following cereals (sorghum, millet) (see e.g. Ripoche et al., (2015). Cattle, goats, and sheep are raised by farmers. Large cattle herds move during the dry season to wetter parts of the country (e.g. *Bougouni, Kadiolo*) due to local lack of feed. The soils at the research station are classified as Lixisols (FAO, 2006). They have a silty sand texture (10% clay) at the surface (0-35 cm), and clay content increases with soil depth (29.4% between 55 and 85 cm) (Table S1). Soil organic carbon is low (<0.1%) (Table 1), pH is about 6 and CEC is less than 3 cmol (+) kg-1 (Traore et al., 2013).

2.2 Experimental design

The experiment was conducted for two consecutive seasons (2017 and 2018) on the same field. Treatments were kept on the same subplots and not re-allocated from a year to another. Two sorghum varieties, namely Tiemarifing (local variety, V1) and 02-SB-F4DT "Grinka" (improved variety for grain production, V2) were cultivated as sole crops, or intercropped with dual-purpose (i.e. grain and fodder production) cowpea IT89KD-245 "Sangaraka". V1 is a photoperiod-sensitive variety, and V2 is less sensitive to photoperiod than V1 (Chantereau, et al., 2013). Sorghum variety and cropping system (sole vs intercrop) were the main treatments. The effect of two sowing dates for sorghum (D1-early sowing, D2-late sowing) was also investigated as a secondary treatment. Sorghum early sowing was done after 15 June (to limit the probability of dry spell occurring after sowing) and after a rainfall greater than 20 mm. Early sowing (D1) occurred on 24 June in 2017 and 26 June in 2018. Late sowing (D2) of sorghum occurred on 20 July in both years. Cowpea was sown two weeks after early- and late-sown sorghum. In 2017, N fertilizer application was 8 kg N/ha. In 2018, two levels of fertilization (F0=0 kgN/ha and F1=38kgN/ha split in two applications) were investigated.

Sole and intercropped sorghum was planted at 0.80 m between sowing rows and 0.40 m along the sowing row. Two sorghum plants per hill were kept, leading to a sorghum density of 6.25 plants m^{-2} in all treatments. An additive intercropping pattern was chosen where cowpea was sown in continuous line between two sorghum plants (on the sorghum row) leading to a cowpea density of 6.25 plants m^2. Weeds were controlled using hand hoe three times for D1 and twice for D2, to keep plots free from weed pressure. Intercropped cowpea did not receive any specific fertilization other than that applied on sorghum. Sole cowpea was cultivated without nitrogen application (F0) in 2018. In 2017 there was no sole cowpea plot. Sorghum stem borer (armyworm) and cowpea pests (e.g. *aphids, Aphis craccivora*) were controlled with chemicals to prevent damage to crops.

The combinations of year, sorghum variety, cropping system, fertilization and sowing date defined 25 cropping situations grown on 25 experimental plots where plant growth and soil characteristics were monitored and used for model calibration and evaluation (Table 1).

2.3 Measurements in experimental plots

2.3.1 Soil measurements

In 2017, a composite sample representing the experimental field was taken at a depth of 0-20 cm before the crops were planted and used to determine soil pH and soil C:N ratio. In 2018, a composite soil sample was taken in each experimental plot with semi-cylindrical augers at a depth of 0-20 cm before crop installation. Theses samples were sun-dried and sent to the laboratory for determination of total soil nitrogen using the Kjeldahl method (Bremner and Mulvaney, 1982) (Table 1).

In 2018, soil volumetric water content was measured with a Diviner 2000 probe placed in vertical access PVC tubes inserted in the soil in each experimental plot. The tubes were installed two weeks before sorghum sowing. The soil-tube interface was carefully filled with fine earth to eliminate gaps at the soil-tube interface, as probe measurements are very sensitive to the quality of the contact between the access tube and the soil (Basinger et al., 2003). The soil was dry at the time of installation, so that the planned maximum depth of 155cm was not reached in some of the experimental plots (the maximum measurement depth in each plot is given in Table 1). Soil water content was measured at 10 cm intervals down to the maximum depth of the tube. Measurements were taken 2-3 times per week from the installation of the tubes to sorghum harvest. Plant-available water across soil profile (i.e. every 10 cm to the maximum depth of the tube) was calculated as the difference between soil water content measured at a given time across the profile and soil water content at wilting point. In each experimental plot, plant available water in the 10-cm layers was aggregated to the maximum depth to obtain total plant available water.

2.3.2 Plant measurements

Date of flowering was recorded for sorghum and cowpea in sole and intercropping plots when 50% of the plants reached the stage. Physiological maturity of sorghum was observed when 100% of the plants had completed the stage of dark spots appearing at the edge of the grain attachment on the panicle. For cowpea, physiological maturity was considered when the first pods started to dry. Leaf Area Index (LAI) was measured using a Licor-LAI2000 (Licor, INC.) on four transects (covering three planting rows) with six plants per transect on each measurement date for sole and intercropped sorghum plots (Fig. S1). Measured LAI on the four transects was then averaged to get the final LAI value for the plot at a given date. LAI measurements began on July 15 and continued until maturity with a 15-day interval between measurements. Seven LAI measurements were made for plots with early sowing (D1) and five for plots with late sowing (D2) of sorghum. Only five LAI measurements were taken under cowpea in sole crop condition, because cowpea senescence started before sorghum. For intercropping there were six LAI measurements in plots with D1 and four measurements in plots with D2. For the first three measurements, only sorghum LAI was measured, because cowpea was too small and the LAI meter could not go under its canopy without direct contact of leaves with the lens. For the remaining measurements, LAI was measured (i) under cowpea canopy (to obtain total canopy LAI, i.e. sorghum and cowpea), and (ii) above cowpea canopy (to estimate sorghum LAI). The LAI of intercropped cowpea was estimated as the difference between the two measurements. Sorghum and cowpea aboveground biomass (stem, leaves and parts of the inflorescence at flowering) was sampled in three randomly selected 1 m^2 quadrats (corresponding to six sorghum stands and six cowpea stands) in each experimental plot every two weeks after crop installation. Fresh samples of sorghum and cowpea were weighted and oven-dried for 48h at 72°C for dry weight estimation. At harvest, yield and yield components were determined: grain yield, grain weight, number of grains, straw weight, thousand seed weight and harvest index for sorghum in 2017 and 2018. For cowpea, grain yield was measured in 2018 in 2017, but in 2017 the sample for dry weight estimation was lost before weighing, so that there was no cowpea grain yield data for 2017. In 2018, cowpea number of grains could not be determined due to

199 destruction of the sub-sample by animals during drying on a dedicated but insufficiently protected area
200 in N'Tarla experimental station. Determination of plant nitrogen content was obtained using the Kjeldahl
201 method (Bremner and Mulvaney, 1982) applied to plant samples taken at flowering (aboveground
202 biomass) and at harvest (bulked stems and leaves, and grains) in all experimental plots.

203

204 **2.3.3 Weather data**

205 Daily climate data for the two growing seasons (2017 and 2018) was obtained from observations at the
206 N'Tarla meteorological station located 50 m from the experimental plots. Measured variables included
207 daily rainfall, daily minimum and maximum temperatures, sunshine duration, and wind speed. Global
208 radiation (*Rg*) was calculated as a function of latitude, maximum possible sunshine duration or daylight
209 hours and solar radiation received at the top of the Earth's atmosphere, using the following equation
210 (usually referred to as Angstrom formula (Allen et al., 1998):

211 $$Rg = [\mathrm{a} + (\mathrm{b}\,\mathrm{x}\frac{n}{N}] \times Ra \qquad (1)$$

212 Where n is the actual sunshine duration measured in hours, N is the maximum daylight duration (Allen
213 et al., 1998). Ra is the extra-terrestrial radiation, i.e. the solar radiation received at the top of the Earth's
214 atmosphere. N and Ra were computed from latitude and date using astronomic formulas, and the
215 coefficients a and b were set at the values 0.25 and 0.50 respectively, as recommended in Allen et al.,
216 1998.

217

218 **2.4 Assessment of the performance of sorghum-cowpea intercropping**

219 Cropping system performance was evaluated for aboveground biomass and grain yield with sole and
220 intercropping, with the computation of Land Equivalent Ratio (LER). LER is the land required with sole
221 cropping to produce the yield obtained with intercropping with the same management (Willey, 1979). It

222 is a commonly used approach to assess the land use advantage associated with intercropping (Willey
223 and Rao, 1980):

224 $$LER = Ya/Sa + Yb/Sb \quad (2)$$

225 Where Ya and Yb are the yields of intercropped sorghum and intercropped cowpea, respectively, and
226 Sa and Sb are the yields of sole sorghum and sole cowpea, respectively.

227 pLERa and pLERb are the partial LER values for each species:

228 $$pLERa = Ya/Sa \quad (3)$$

229 $$pLERb = Yb/Sb \quad (4)$$

230 A LER value greater than 1 indicates that there is an advantage for intercropping over sole cropping.
231 Partial land equivalent ratio (*pLER*) values are used to assess the contribution of each crop to the final
232 LER.

233 **2.5 General description of STICS soil-crop model**

234 STICS soil-crop model (Brisson et al., 2009) simulates carbon, water and nitrogen balances in the soil-
235 crop-atmosphere system. The model simulates the dynamics of agricultural and environmental variables
236 (e.g. crop yield, N in harvested organs, soil moisture and mineral N content, nitrogen leaching and soil
237 organic carbon) over agricultural seasons on a daily time step, taking into account the impact of
238 weather, and soil and crop management practices (e.g. mineral and organic fertilization, irrigation, tillage
239 and residue management). It has been designed as a generic model that can be easily adapted to
240 different crops and environmental conditions. Crops are defined using eco-physiological options (e.g.
241 effect of photoperiod and/or the requirements of cold on crop phenology) and plant parameters. Plant
242 parameters include both crop specific and cultivar-dependent parameters. The version of the model
243 used for this study is the intercropping extension of the STICS sole crop model that can consider two
244 species grown at the same time (Brisson et al., 2004). This model, hereafter referred to as "Stics-

intercrop" simulates the competition for light, water and nitrogen between intercropped species at a daily time step (Brisson et al., 2004). In the following section, we describe the general functioning of Stics, and detail the specific features of Stics-Intercrop.

2.6. Description of Stics model and intercrop version specificities

Plant development occurs in several stages associated with LAI and phenological stages (Table 2). The duration between stages is expressed in cumulative thermal time and is specific to species and varieties. Development is controlled by crop temperature (simulated variable). Germination and emergence are controlled by soil temperature and moisture.

Crop height varies during growth, using a function relating height to LAI, and is limited to a maximum value for each species (*hautmax* parameter). In the intercropping version, the comparative height of the two crops determines the dominant and the understory (i.e. dominated) plant. The model is thus able to simulate possible inversions in dominance between the two species during crop cycle. The sole-crop model uses Beer's law to compute radiation interception. Stics-intercrop differs on that aspect and uses a "Radiative transfer" formalism to compute radiation interception: the model estimates direct and diffuse radiation received each day for 20 points uniformly distributed along the inter-row, and the fractions intercepted by the foliage of the dominant crop and transmitted to the layer below (Brisson et al., 2009)**.** Each crop has a single extinction coefficient (*ktrou*, the same for direct and diffuse radiation). Row spacing (*interrang* parameter), row orientation (*orientrang* parameter) and canopy volume impact radiation transfers. The canopy volume is defined by (i) basic shapes (*form* parameter, either triangle or rectangle), (ii) a ratio between the height and width of the shape (*rapform* parameter), and (iii) the base height of the shape *(hautbase* parameter), considering absence of leaves between zero and base height (Brisson et al., 2004). The shape and the base height are assumed to be constant throughout crop cycle. Width varies as a function of height, distance between plant rows, LAI, leaf density distribution as a function of height, and the *rapform* parameter. For each intercropped species, daily LAI is calculated

as a function of crop temperature, phenological stage, plant density, and water and nitrogen stress. The LAI growth phase follows a logistic curve as a function of thermal time. Aboveground biomass daily growth is computed by multiplying the intercepted radiation by a potential radiation use efficiency factor that depends on the species and crop development phase (i.e. juvenile, vegetative and reproductive stages). Root growth is decoupled from aboveground biomass growth. Root front growth and root density are computed as a function of soil temperature, soil moisture and bulk density. Roots absorb water and mineral nitrogen but allocation of biomass to root is not explicitly simulated. Water and nitrogen uptake in intercropping is calculated in STICS according to root density of each crop. Root densities above 0.5 cm/cm^{-3} of soil are not taken into account for water and nitrogen uptake since above this threshold, water and nitrogen uptake are assumed not to be limited by root density (Corre-Hellou et al., 2009). The simulated descent of root front is driven by thermal time using soil temperature with a species-specific rate. Soil moisture content below wilting point or above field capacity can reduce or stop root front growth. Root length growth is calculated by a logistic function similar to that of leaf growth. Roots are distributed in the profile as a function of (i) the amount of roots already present and(ii) soil constraints (drought, anoxia, penetrability). Differing with the sole crop version that uses a single crop coefficient, Stics-intercrop computes the water requirements of the two species with a resistive schemes applied at a daily time step to account for microclimatic effect (e.g. transfer of heat below the dominant plant, see Brisson et al. (2004) for more details). The soil environment is assumed to be the same for both crops, i.e. the horizontal heterogeneity of soil is ignored (but vertical heterogeneity is accounted for). The interactions between the two root systems result from the influence of the soil on the root profile of each crop through its penetrability and water dynamics. Soil supply is determined by the balance between inputs (including possible capillary rise) and losses (soil evaporation, runoff and drainage).

Water stress and nitrogen stress that affect plant growth and grain yield are taken into account in the model using indices of reduced leaf growth and biomass accumulation under water or nutrient limiting

conditions (Brisson et al., 2009). Potential transpiration is a function of Leaf Area Index (LAI) and daily potential evapotranspiration. The latter is as calculated using the approach of Shuttleworth & Walace (Brisson et al., 1998). Actual transpiration is calculated as the minimum between soil water supply and maximal crop demand. The water stress factor that affects radiation use efficiency and plant transpiration is calculated as the root transpirable fraction of soil water, which reduces growth and transpiration (Brisson et al., 2009). Daily plant nitrogen accumulation depends on biomass accumulation and soil nitrogen availability. Nitrogen uptake for each species depends on root depth, root distribution in soil layers and crop nitrogen demand. Daily nitrogen demand is the product of plant growth rate by the N amount corresponding to maximum N dilution in the plant. Soil supply is calculated per 1 cm elemental layer up to maximum root system depth. The nitrogen stress factor affects (i) LAI, (ii) radiation use efficiency and (iii) senescence. The N stress factor is calculated as the ratio between actual nitrogen concentration and critical nitrogen concentration in the crop if the former is lower than the latter, and is set to one otherwise. Stress factors are calculated daily and vary between zero (complete stress) and one (no stress). A complete description of the equations and parameters governing stresses definition can be found in Brisson et al. (2008). STICS also simulates N acquisition by N_2 fixation in the case of legume crops. Potential symbiotic N_2 fixation by legumes is a function of nodule life cycle and plant growth rate. Actual fixation depends on inhibitory effect related to sub-optimal temperature, soil moisture, and/or excess of nitrate in soil (Brisson et al., 2008).

2.7. Model parameters, model calibration and evaluation

Growing seasons and the experimental treatments (cropping system, sowing date, sorghum variety and fertilizer input) defined 25 cropping situations (8 in 2017 and 17 in 2018) corresponding to the experimental plots listed in Table 1. Each experimental plot corresponds in this study to a "simulation

unit". The 17 simulation units of 2018 were used for model calibration. The remaining 8 simulations units of 2017 were used for independent model evaluation.

2.7.1 Setting of model parameters

Soil parameters

We defined five horizons for soil parameterization: 0-15cm, 15-35cm, 35-55cm, 55-85cm, and from 85 to maximum sampling depth (that varied per experimental plot, see Table 1). Soil analysis carried-out in the experimental plots (see section 2.3.1) informed the soil parameters “norg” (soil total Nitrogen in the topsoil) (**Table 1**). pH and soil C:N ratio were set constant across all experimental plot to 5.8 and 13, respectively, in line with the soil analysis carried out across all experimental plots in 2017. Soil moisture at field capacity and wilting point were first estimated with pedo-transfer functions (Lidon and Francis, 1983) based on the texture measured in 2017 in a soil profile in one location close to the experiment **(Table S1).**

Plant parameters

Model parameters related to crop geometry reflect the assumption that the two species in the intercrop occupy distinct rows. In our experimental design, cowpea was planted on the same row as sorghum. This mismatch between reality and model assumptions was easily overcome by considering that the spacing between plants on a given row was the spacing between rows, and that the spacing between rows was the spacing between plants on a given row (see Fig S2).

Model parameters related to grain yield formation were directly derived from the measurements made in the experimental plots (Table 3). The greatest experimental value of grain weight among the 16 experimental plots was considered to inform the parameter that set maximum number of grains (*nbgrmax*). Maximum height (*hautmax*) was set as measured after flowering in the experiment, i.e. 4 m for sorghum and 0.5 m for cowpea. A few other parameters were taken from the literature (e.g. temperature thresholds for development and photosynthesis) (Table 3).

2.7.2 Calibration procedure

STICS model has not been previously calibrated for cowpea and tropical sorghum. Initial parameter values for cowpea were obtained from the spring pea plant file (Corre-Hellou et al., 2009). For sorghum, initial parameters were taken from the STICS sorghum plant file as obtained with the 8.5 version of the model, which corresponds to temperate fodder sorghum (Constantin et al., 2015). For sorghum, we calibrated cultivar-dependent parameters for the two varieties used in the experiment.

To calibrate the thermal constants associated with development stage, the model was forced to go through the observed dates of maximum leaf area index, flowering and maturity, in order to compute the temperature sums corresponding to the intervals between the stages. We assumed that flowering coincided with the beginning of grain filling. Parameters related to photoperiod (*phobase and phosat*) for the two sorghum varieties (V1 sensitive to photoperiod and V2 less sensitive to photoperiod) were set according to Traore (2015). Phobase and phosat are daylength thresholds that define the period of crop growth during which a photoperiod slowing effect is applied to crop development. Photoperiod sensitivity Index (*sensiphot*) was obtained by trial-and-error to minimize the gap between observed and simulated flowering date (Table 3).

LAI is a central state variable in the model. Parameter related to leaves development (*dlaimax*) was adjusted by trial-and-error to minimize the difference between observed and simulated LAI. Similarly aboveground biomass growth parameters (*efcroijuv, efcroiveg, efrcoirepro*) were also adjusted by trial and error to minimize the difference between the observed and simulated aboveground biomass. The radiative transfer parameter "*ktrou*" used for radiation transfer from sorghum to cowpea was set to 0.30 for sorghum. This value was obtained using a trial-and-error calibration method to minimize the differences between observed and simulated sorghum and cowpea biomass in simulation units with intercropping. Default values for shape and base height (*shape, hautbase* parameters) as well as the ratio between the thickness and width of the crop shape (*rapform* parameter) were considered.

The fraction of stable organic nitrogen in soil (*finert*) was set to zero. This appeared necessary for the model to simulate amounts of soil mineral N and plant nitrogen uptake consistent with the observed crop N uptake in the treatments without fertilization. The moisture at field capacity and at wilting point, that were first set with the help of pedo-transfer functions (see section 2.7.1) were then adjusted for each experimental plot (see final values in Table 1) to minimise the difference between observed and simulated soil water during the growing season.

For some parameters the simple trial and error approach used above would have been poorly effective and we used instead the optimization tool implemented in the software package associated with Stics model (Table 3). This optimizer proposes a parameter values that minimizes the gap between model simulation and observations for the variables to be explained (Buis et al., 2011), using weighted least squares (Makowski et al., 2006). Lower and upper parameters limits were set before optimization to ensure that the optimized values correspond to reasonable physiological values. Crop parameters were first calibrated using sole sorghum and cowpea simulation units. Then, these parameters were refined using intercropping simulation units. The parameters Kmabs2 (*i.e.* the affinity constant of N uptake by the roots for the low uptake system) and Vmax2 (i.e. the maximum specific N uptake rate with the high affinity transport system) were optimized to minimize the difference between observed and simulated plant N uptake. Parameters related to grain formation such as the slope of the relationship between grain number and growth rate (*cgrain*), the number of grains produced when growth rate is zero (cgrainv0) were also optimized by minimizing the difference between the simulations and the observations of the number of grains (Table 3). The rate of increase of the harvest index vs. time (*viticarbT*) was adjusted to minimize the difference between simulations and observations for grain yield.

2.7.2 Model evaluation

Model error was estimated with the root means square error (*RMSE)*, which has the same unit as the considered variable, and its relative value in % (*rRMSE*). We used these statistical criteria to assess the

accuracy of STICS simulations for maximum leaf area index (*Laimax*), aboveground biomass, plant N uptake and grain yield of sole and intercropped sorghum and cowpea.

$$RMSE = \sqrt{\frac{1}{n}\sum_{i=1}^{n}(Oi - Si)^2} \quad (5)$$

$$rRMSE = \frac{RMSE}{\bar{O}}\ X\ 100 \quad (6)$$

Where O_i et S_i are the observed and simulated values for the ith measurement, n is the number of observations and $\bar{O}$ is the average of the observed values.

Model efficiency (*EF*) was also calculated:

$$\mathrm{EF} = 1 - \frac{\sum_{\mathrm{i}=1}^{\mathrm{n}}(\mathrm{Oi} - \mathrm{Si})^2}{\sum_{\mathrm{i}=1}^{\mathrm{n}}(\mathrm{Oi} - \bar{\bar{O}})^2} \quad (7)$$

Model efficiency (EF) (Willmott et al., 1985) varies from infinite negative value to 1 (perfect performance). A negative value indicates that the mean of observations is a better predictor than the model, and a zero value indicates that the model does not outperform the mean of observed values. The combined analysis of these three indicators gives a comprehensive assessment of model accuracy.

3. Results

3.1 Weather data

Compared to that of 2018, growing season in 2017 was cooler and wetter in terms of cumulated rainfall, but with a greater number of dry days and greater solar radiation overall. The average minimum temperature observed in 2017 (17.3°C) was 5°C lower than that observed in 2018 (22.3°C) during the growing season (Figure 1). Average Maximum temperature in 2017 (34.2°C) was 2.1°C lower than average maximum temperature in 2018 (36.3°C). Average growing season temperature in 2017 (27.9°C) was 1.1°C lower than in 2018 (30.0°C). Average global solar radiation during the growing season in 2017 (23.1 MJ m^{-2}) was greater than in 2018 (18.0 MJ m^2). Cumulative rainfall recorded in

2017 (808 mm) (Fig. 1A) was 110 mm greater than in 2018 (698 mm) (Fig. 1B). On the other hand, there were more dry days (i.e. days with no rainfall) in 2017 (134 days) than in 2018 (122 days).

3.2. Model calibration

3.2.1. Sorghum and cowpea phenology

Model simulations of sorghum phenology led to a RMSE of 3.4 days for beginning of grain filling and 3.1 days for physiological maturity (Fig. 2a, 2b). RMSE for cowpea phenology was 3.9 days for grain filling and 10.8 days for physiological maturity (Fig. 2a, 2b).

The model reproduced the relatively high sensitivity of V1 to photoperiod reasonably well: a 24-day delay in sowing (i.e. the difference between early and late sowing in the experiments) shortened the observed length of the vegetative phase (from planting to start of grain filling) by 17 days. The model simulated a 14-day decrease in the length of vegetative phase when sowing was delayed. V2 was less sensitive to photoperiod: a 24-day delay in sowing created only a 9-day observed shortening of the vegetative phase. The model simulated a 6-day decrease in the length of the vegetative phase when sowing was delayed.

3.2.2. Simulation of in-season soil water, LAI and aboveground biomass (AGB)

Sole crops with calibration dataset

In-season soil water was well reproduced by the model, especially the increase in soil water up to field capacity during vegetative phase (Fig. 3). However, soil water after the end of the growth cycle (a period with low rainfall and high soil evaporation) was overestimated by the model due to the underestimation of soil evaporation.

A reasonably good agreement between model and observations for the key plant growth variables was reached after calibration. However, it was not possible to calibrate LAI and biomass growth with an equally satisfactory fit for the two sowing dates treatments and the two sorghum cultivars (Fig. 3). For

sole sorghum with early sowing date (D1) and nitrogen input (F1), LAI simulated by model matched the observations for the improved variety (V2) and slightly overestimated them for the local variety (V1) (Fig. 3a, 3c). With late sowing (D2) and nitrogen input (F1), the model overestimated observed maximum LAI for both sorghum varieties (Fig. 3b, 3d). With early sowing (D1) and without nitrogen input (F0), the model overestimated observed LAI for V1 (Fig. 3e) but agreed with observed LAI for V2 under the same fertilization conditions (Fig. 3g). With late sowing (D2) and without nitrogen input (F0), the model overestimated LAI for both sorghum varieties (Fig. 3f, Fig. 3h). LAI simulations for cowpea in sole crop matched closely the observations (Fig. 3i).

AGB was underestimated (especially around flowering) in simulations for both sorghum varieties with early sowing (D1) and N input (F1) (Fig. 3a, Fig. 3c). With late sowing (D2) and N input (F1), AGB simulations were in closer agreement with in-season and harvest observations for V1 and V2 (Fig. 3b, 3d). Without nitrogen supply (F0), the same trends were observed for early sowing i.e. sorghum AGB was overestimated for both varieties (especially around flowering) (Fig. 3e, 3g) but underestimated at harvest for late sowing (Fig. 3f, 3h). The simulation of cowpea AGB closely matched the observation (Fig. 3i).

Intercrops with calibration dataset

Simulated in-season soil water for intercrops corresponded fairly well to the observations (Fig.4 a, 4b, 4c, 4d, 4m, 4n, 4o, 4p). As with sole crops, soil water at the end of the season was overestimated. Simulated LAI of (i) total canopy (sorghum plus cowpea), (ii) sorghum, and (iii) cowpea matched the observations for variety V2 (Fig. 4q) but model simulations overestimated the observations for variety V1 (Fig. 4e) with early sowing (D1) and nitrogen input (F1). With late sowing (D2) and nitrogen input (F1), the model overestimated LAI of i) total canopy (sorghum and cowpea), (ii) sorghum, and (iii) cowpea for V1 and V2 (Fig 4f, 4r). Without N input (F0), the model also overestimated the LAI of (i) total

canopy (sorghum and cowpea), (ii) sorghum, and (iii) cowpea for the two sorghum varieties, in early and late sowing (Fig. 4g, 4s, 4h, 4t).

With early sowing (D1) and nitrogen input (F1), the model underestimated sorghum AGB throughout crop cycle for V1 (Fig. 4i), and matched more closely the observations for V2 (Fig 4u). With late sowing (D2) and nitrogen application (F1), AGB simulations matched the observations for both sorghum varieties (Fig. 4j, 4v). With early sowing (D1) and without nitrogen input (F0), the model simulated accurately AGB throughout crop cycle for V1 and V2 (Fig 4k, 4w). With late sowing (D2) and without nitrogen input (F0), the model overestimated sorghum AGB at the end of crop growth (Fig. 4l, 4x). For cowpea, the model accurately simulated AGB throughout the crop cycle whether grown with V1 or V2, with and without N inputs (Fig. 4i, 4u, 4j, 4v, 4k, 4w, 4l, 4x).

Sole and intercrops in evaluation dataset

In sole and intercropping conditions, though the soil was filled with water during crop early growth, water stocks rapidly decreased below 50% of maximum available plant water capacity, indicating possible water stress (Figure S3 and Figure S4). For all sowing dates, for sole crops and intercrops, model simulations overestimated observed LAI (Fig. S3, Fig. S4). For sole crops, AGB simulations were in close agreement with the observations during the season but overestimated the observations at harvest for the local variety (V1) regardless of sowing dates (Fig. S3a, S3b). For the improved variety (V2), model simulations of AGB were in good agreement with observations (Fig. S3c) for early sowing. With late sowing, AGB was overestimated at the end of the cycle (Fig. S3d). With intercropping, AGB simulation displayed similar trends as observed with sole cropping (Fig. S4, e, f, k, l).

3.2.3 Simulation of aboveground biomass, plant N, number of grains and grain yield at harvest

Sorghum and cowpea AGB at harvest varied widely in sole cropping and intercropping, due to differences in sorghum variety, sowing date and fertilizer inputs: aboveground biomass ranged from 3.5

t/ha to 9.6 t/ha for sorghum and from 0.4 t/ha to 2.5 t/ha for cowpea for the calibration dataset. The model reproduced this variability with rRMSE of 23 % and EF of 0.81 (Fig. 5a, Table 4). EF of model simulation was smaller in evaluation compared with calibration (Table 4), and rRMSE was greater, indicating a loss in the accuracy of model simulation of AGB with the independent calibration dataset.

The model underestimated plant N at harvest (Fig. 5c): rRMSE was 35% and EF was negative (-0.05). With regard to grain number per m^2 of sorghum (Fig. 5e), rRMSE was 29% (Table 4), and remained fairly stable with evaluation dataset (rRMSE = 25%). The variability in observed grain yield across crops and experimental treatments was well reproduced by the model (Fig. 5g). Although rRMSE was large (49%), EF was 0.56 (Table 4, Fig.5). Model accuracy in simulating grain yield remained fairly stable with the evaluation dataset (rRMSE = 14% with the evaluation dataset), though EF became negative (Table 4).

3.3 Simulation of the impact of intercropping, fertilizer and variety on crop yield and LER

Observed sorghum and cowpea grain yield decreased with intercropping compared with sole cropping (see figure 6a, 6c). The model accurately depicted this trend (see Figure 6b, 6d), though it underestimated the greater negative impact of intercropping that was observed for cowpea grain yield. In the experiment, the improved variety (V2) outperformed the traditional variety (Figure 6e) for grain yield, whereas the two varieties did not show marked differences in AGB yield (Figure S5e). The model successfully simulated this trend (Figure 6f). AGB of sorghum increased with N input, but not cowpea biomass (see Figure S5i, k), and this trend was also adequately represented by the model (Figure S5j, l). Grain yield of sorghum also increased with N input, while cowpea yield decreased with N input (Figure 6i, 6k), and this was also well depicted by the model, although the model overestimated

sorghum and cowpea grain yield with no N input (Figure 6j, 6l). AGB and grain yield of sorghum and cowpea decreased with late sowing compared with early sowing (Figure 6m, 6o). The model failed to reproduce such a drop in yield with late sowing (see Figure 6n, Figure 6p). AGB and grain yield of cowpea and sorghum were smaller in 2017 than in 2018 (Figure 6q, 6s and Figure S5q, S5s). The model reproduced such behaviour, although the simulated effect of year on the AGB and grain yield of cowpea and sorghum was less marked than in the reality (Fig 6r, 6t and Figure S5r, S5t).

There was an interaction between cropping system (sole vs intercropping) and growing season. In 2017, the observed negative impact of intercropping on sorghum yield was weaker than in 2018 (Fig S6). The model failed in reproducing such effect and it simulated a more pronounced detrimental effect of intercropping on sorghum yield in 2017 than in 2018. In 2018, the model attributed sorghum and cowpea yield decrease with intercropping to competition for nitrogen: while water stress was identically inexistant in sole- and intercropping, the simulated N stress for sorghum during reproductive phase was stronger (i.e. lower indicator value) in intercropping than in sole cropping (see Figure S7). In 2017, the model simulated a relatively strong water stress during reproductive stage for both intercropping and sorghum sole crop, but this did not impacted LAI as strongly as in the reality and translated into a strong simulated yield reduction only in the intercropping situation whereas the simulated yield of sole sorghum was at the same level as in 2018 where no water or nitrogen stress was simulated (Figure S6, S7).

Despite the decrease in both sorghum and cowpea yield with intercropping (i.e. partial LER below one), overall observed intercropping LER was always above one, with regard to AGB (Figure 7A). The model proved accurate in simulating this behavior, as simulated LER was always above one (Figure 7B). Decrease in observed cowpea AGB with intercropping was greater than the decrease in sorghum AGB, and the model was satisfactorily depicting this trend. With regard to grain yield, LER was above one without N input, and below one with N input (due to a stronger decrease in cowpea grain yield) (Figure

535 7C). Because the model did not capture the stronger decrease in cowpea grain yield with N input and
536 intercropping, the simulations could not reproduce these LER values below one (Figure 7D).
537
538 **4. Discussion**
539
540 *Promising features of the calibrated model*
541 The calibrated intercrop model reproduced the key feature of the tested additive intercropping: LER for
542 AGB was always above one, thanks to a moderate decrease in sorghum ABG and despite a more
543 pronounced decrease in cowpea AGB. This decrease is cowpea AGB with intercropping was probably
544 linked to the competition for solar radiation that is primarily intercepted by sorghum canopy. This gives
545 confidence in the ability of the Stics intercrop model to predict the behaviour of intercropping based on
546 two plant species with contrasting heights. Chimonyo et al., (2016) found a similar promising feature of
547 the APSIM model.
548 The grain yield advantage of the improved variety over the local variety, and the yield advantage of N
549 input over no fertilization, were also fairly well simulated. The model simulated less accurately but
550 reasonably well the observed differences in yield resulting from the differences in water stress
551 occurrences between our two experimental years, under intercropping conditions. The model can help
552 identify complex interactions between growing season characteristics, N inputs, and the competitions at
553 stake in the intercropping system. While competition for water clearly prevailed in the intercropping
554 situations of 2017, the simulations suggested that competition for nitrogen occurred in the intercropping
555 situations in 2018, with clearly less water stress. Such competition for nitrogen can be surprising -
556 because cowpea is a legume that fixes atmospheric nitrogen. Cowpea did fix nitrogen in the experiment.
557 The observed N uptake for sole sorghum without N fertilizer was 90 kgN/ha (i.e which indicates that at
558 least 90 kgN/ha was provided by the mineralization of soil organic matter). Sole cowpea with no fertiliser
559 input achieved a N uptake above 200 kgN/ha. This indicates a possible N_2 fixation of at least 110 kgN
560 ha^{-1} (on top of the 90 kg N/ha provided by the soil organic matter mineralisation). However, N

competition can still occur when mineral fertilizer are applied. High level of soil mineral N can depress the amount of atmospheric N_2 that is fixed by the legume (Sprent et al., 1988). This decrease in legume N_2 fixation with mineral fertilizer input has been observed in wheat-pea and barley pea-experiments (Bedoussac and Justes, 2010; Corre-Hellou et al., 2009), and this process is accounted for by the Stics model (Brisson et al., 2009). Detailed measurement of the amount of N_2 fixed by the legume (using ^{15}N natural abundance method), in sole and intercropping, would be required to validate this simulated competition for nitrogen in 2018.

Avenues to improve model calibration

Despite the promising features of the model, prediction error of crop AGB and grain yield remained rather large (in the range 29-49%), compared with other studies. Chimonyo et al. (2016) obtained rRMSE values for grain yield and aboveground biomass in the range 6-15% when simulating sorghum-cowpea intercropping in South Africa. Masvaya (2019) obtained rRMSE for grain yield in the range 18-29% when simulating grain yield of sorghum and cowpea with sole and intercropping in semi-arid Zimbabwe.

In this study, the calibrated intercrop model failed to accurately predict the low yield of cowpea with intercropping, and thus overestimated LER for grain. In Stics, the number of grain (a key yield component) is determined by biomass growth during a short period before the beginning of grain filling (Falconnier et al., 2019). Accurately setting the length of this period, and set the parameters that define the relation between biomass growth and the final number of grain requires measurement of biomass growth during that period, along with measurement of the final number of grain, for a range of contrasting experimental conditions (e.g. with/without water and nitrogen stress) (Affholder et al., 2013). The latter was missing in our experimental setting, and more detailed measurement of biomass growth and grain number would certainly be necessary to improve model accuracy. The resulting robustness of yield prediction under water stress during reproductive stage was insufficient to predict correctly the

impact of water stress in some cropping situations. Caution should therefore be taken in the interpretation of the simulated inter-annual variation in grain yield of intercropping when using historical weather records and/or future climatic series. The model also overestimated grain yield of sorghum and cowpea with no N input. This is possibly related to the poor simulation of N uptake by both sorghum and cowpea. Measurement of initial soil mineral N prior to sowing and during crop growth would possibly help improve the calibration of the mineralization of soil organic matter and crop N uptake. These improvements in model calibration with regard to yield component and yield with no N input are required to improve our confidence in the prediction of LER for grain. This will be crucial if the model is to be used for virtual experiments where sustainable intensification pathways with intercropping are tested.

Late planting of sorghum resulted in smaller yield, and the model could not reproduce this behaviour. Late sowing of photoperiodic plant decrease the length of their growing cycle, thus directly lowering the amount of radiation intercepted and the final yield (Tovignan et al., 2016). Such effect should be smaller with the less-photoperiodic variety for which late planting does not translate into shorter growing cycle. But the improved variety was also impacted by late sowing. Possibly, the late plantings were negatively impacted by excess water in the plots (anoxia), a process that can be taken into account by the Stics model, but that we did not calibrate due to lack of appropriate data on soil water conductivity under saturated conditions. Low nitrogen availability due to runoff (sowing during the period of intensive rainfall), or armyworm damage on sorghum could also possibly contribute to the discrepancy between observations and model simulations. Armyworm damage was observed on sorghum plants during the 2018 season but their impact on yield was not assessed. The Stics model does not simulate the impact of pests on the crop.

A calibrated intercrop model to explore options for sustainable intensification in land constrained sub-Saharan Africa

Our experimental design investigated the crucial features of sustainable intensification, namely the integration of legumes with intercropping, the use of mineral fertilizer, combined with improved varieties (Vanlauwe et al., 2014). The calibrated intercrop model was able to mimic the key main effects and interactions at play when investigating the performance of these options. Hence, it can be a crucial tool to explore pathways toward sustainable intensification of agriculture in land constrained sub-Saharan Africa. Intercropping is generally a better option with low fertilizer inputs (Bedoussac et al., 2015; Yu et al., 2015). Our experimental results also support such claim. This contrasts with the now widely acknowledged need for sustainable intensification of agriculture with more mineral fertilizer in sub-Saharan Africa (Jayne et al., 2018). The predicted increase in climate variability and climate change in sub-Saharan Africa (Sultan and Gaetani, 2016) may alter such picture, as intercropping is also well known to stabilize yield (Weih et al., 2021). Crop models and crop models ensembles are great tools to investigate the interactions between crop management and climate variability and change in sub-Saharan Africa (Falconnier et al., 2020). The increasing availability of promising calibrated intercrop model (e.g. this study, Chimonyo et al. (2016); Masvaya (2019)) offer the prospect of ensemble simulation of the performance of intercropping in the face of climate variability and change, in order to guide the design of adaptive cropping system involving intercropping.

5. Conclusion

Our study showed that the locally calibrated intercropping version of the STICS soil-crop model displayed some promising features to explore the performance of sorghum-cowpea intercropping under tropical rainfed environment. In the experiment, sorghum and cowpea aboveground biomass and yield decreased with intercropping compared with sole cropping, but observed LER for aboveground biomass remained above one, regardless of experimental treatment (fertiliser, sowing date and sorghum variety). The calibrated model accurately depicted this overall trend related to LER for aboveground biomass, and satisfactorily accounted for the impact of fertiliser and sorghum variety. It can therefore be a useful

636 tool to understand the competitions that occur between the intercropped species in this additive cereal-
637 legume intercropping systems in tropical rainfed environment, under the framework of sustainable
638 intensification and integrated soil fertility management. Despite this promising feature of the model,
639 large inaccuracies in the simulated leaf area index and N uptake were observed. The detrimental impact
640 of late sowing on sorghum yield, possibly because of anoxia, was also poorly accounted for. Though the
641 model can be used to explore the impact of inter-annual climate variability on intercropping
642 performance, these limitations will constraint the ability of the model to accurately and meaningfully
643 portray the interactions at stake when crop management varies strongly. We therefore advocate for
644 increased, continuous and detailed experimental effort on cereal-legume intercropping systems (e.g.
645 measurement of soil mineral N, N_2 fixation, and grain number for a great range of contrasted cropping
646 situations), in order to improve the calibration of parameters related to water and N stress. This will
647 improve model ability to deal with intercropping, a key management option for sustainable intensification
648 of smallholder farming in the global South.

649 **Acknowledgement:**

650 The Agriculture and Climate Risk Management program: Tools and Research in Africa "Agricora" and
651 the "Eco-Fert-Clim" project funded the field work of this study. The authors are grateful to Remi Vezy
652 who provided useful scripts and R functions that greatly help analyze simulation outputs, and also to
653 Eric Justes for useful insights on intercrop model calibration.

654

655 **Reference**

656 Affholder, F., Parrot, L., Jagoret, P., 2014. Acquis et perspectives de l'intensification écologique, in:
657 Sourrisseau, J.-M. (Ed.), Agricultures familiales et mondes à venir. Versailles, France, pp. 303–
658 316.
659 Affholder, F., Poeydebat, C., Corbeels, M., Scopel, E., Tittonell, P., 2013. The yield gap of major food
660 crops in family agriculture in the tropics: Assessment and analysis through field surveys and
661 modelling. Field Crops Res. 13.
662 Allen, R.G., PEREIRA, L.S., RAES, D., SMITH, M., 1998. Crop evapotran-spiration-Guidelines for
663 computing crop water requirements-FAO Irrigation and Drainage Paper N° 56. FAO 1–15.

664 Andrews, D.J., Kassam, A.H., 1976. The Importance of Multiple Cropping in Increasing World Food
665 Supplies, in: Papendick, R.I., Sanchez, P.A., Triplett, G.B. (Eds.), ASA Special Publications.
666 American Society of Agronomy, Crop Science Society of America, and Soil Science Society of
667 America, Madison, WI, USA, pp. 1–10. https://doi.org/10.2134/asaspecpub27.c1
668 Baldé, A.B., Scopel, E., Affholder, F., Corbeels, M., Da Silva, F.A.M., Xavier, J.H.V., Wery, J., 2011.
669 Agronomic performance of no-tillage relay intercropping with maize under smallholder
670 conditions in Central Brazil. Field Crops Res. 124, 240–251.
671 https://doi.org/10.1016/j.fcr.2011.06.017
672 Basinger, J.M., Kluitenberg, G.J., Ham, J.M., Frank, J.M., Barnes, P.L., Kirkham, M.B., 2003. Laboratory
673 Evaluation of the Dual-Probe Heat-Pulse Method for Measuring Soil Water Content. Soil Sci.
674 Soc. Am. 2, 389–399. https://doi.org/10.2136/vzj2003.3890
675 Bedoussac, L., Journet, E.-P., Hauggaard-Nielsen, H., Naudin, C., Corre-Hellou, G., Jensen, E.S., Prieur,
676 L., Justes, E., 2015. Ecological principles underlying the increase of productivity achieved by
677 cereal-grain legume intercrops in organic farming. A review. Agron. Sustain. Dev. 35, 911–
678 935.
679 Bedoussac, L., Justes, E., 2010. The efficiency of a durum wheat-winter pea intercrop to improve yield
680 and wheat grain protein concentration depends on N availability during early growth. Plant
681 Soil 330, 19–35. https://doi.org/10.1007/s11104-009-0082-2
682 Bonny, S., 2011. Ecologically intensive agriculture: Nature and challenges. Cah. Agric. 20, 451–462.
683 https://doi.org/10.1684/agr.2011.0526
684 Boote, K.J., Jones, J.W., Pickering, N.B., 1996. Potential Uses and Limitations of Crop Models. Agron.
685 J. 88, 704–716. https://doi.org/10.2134/agronj1996.00021962008800050005x
686 Bremner, J.M., Mulvaney, C.S., 1982. Nitrogen-Total, in: Klute, A. (Ed.), Methods of Soil Analysis Part
687 2. American Society of Agronomy, Soil Science Society of America, Madison, WI, USA, pp.
688 595–624. https://doi.org/10.2134/agronmonogr9.2.2ed.c31
689 Brisson, N., Bussière, F., Ozier-Lafontaine, H., Tournebize, R., Sinoquet, H., 2004. Adaptation of the
690 crop model STICS to intercropping. Theoretical basis and parameterisation. Agron. EDP Sci.
691 24, 409–421. https://doi.org/10.1051/agro:2004031. hal-00886023
692 Brisson, N., Launay, M., Mary, B., Beaudoin, N., 2009. Conceptual Basis, Formalisations and
693 Parameterization of the Stics Crop Model. Editions Quae, Paris.
694 Brisson, N., Mary, B., Ripoche, D., Jeuffroy, M.H., Ruget, F., Nicoullaud, B., Gate, P., Devienne-Barret,
695 F., Antonioletti, R., Durr, C., Richard, G., Beaudoin, N., Recous, S., Tayot, X., Plenet, D., Cellier,
696 P., Machet, J.-M., Meynard, J.M., Delécolle, R., 1998. STICS: a generic model for the
697 simulation of crops and their water and nitrogen balances. I. Theory and parameterization
698 applied to wheat and corn. Agronomie 18, 311–346. https://doi.org/10.1051/agro:19980501
699 Buis, S., Wallach, D., Guillaume, S., Varella, H., Lecharpentier, P., Launay, M., Guérif, M., Bergez, J.-E.,
700 Justes, E., 2011. The STICS Crop Model and Associated Software for Analysis,
701 Parameterization, and Evaluation, in: Ahuja, L.R., Ma, L. (Eds.), Advances in Agricultural
702 Systems Modeling. American Society of Agronomy and Soil Science Society of America,
703 Madison, WI, USA, pp. 395–426. https://doi.org/10.2134/advagricsystmodel2.c14
704 Carsky, R.J., Douthwaite, B., Manyong, V.M., Sanginga, N., Schulz, S., 2003. Amélioration de la gestion
705 des sols par l'introduction de légumineuses dans les systèmes céréaliers des savanes
706 africaines. Cah. Agric. 12, 227–233.
707 Cassman, K.G., 1999. Ecological intensification of cereal production systems: Yield potential, soil
708 quality, and precision agriculture. Proc. Natl. Acad. Sci. 96, 5952–5959.
709 https://doi.org/10.1073/pnas.96.11.5952
710 Chantereau, J., François Cruz, J., Ratnadass, A., Trouche, G., 2013. Le Sorgho, Quæ,. ed. CTA, Postbus
711 380, 6700 AJ Wageningen, Pays-Bas, Versailles-Gembloux.
712 Chimonyo, V.G.P., Modi, A.T., Mabhaudhi, T., 2016. Simulating yield and water use of a sorghum–
713 cowpea intercrop using APSIM. Agric. Water Manag. 177, 317–328.
714 https://doi.org/10.1016/j.agwat.2016.08.021

715 Connolly-Boutin, L., Smit, B., 2015. Climate change, food security, and livelihoods in sub-Saharan
716 Africa. Clim. Change 385–399. http://dx.doi.org/10.1007/s10113-015-0761-x
717 Constantin, J., Willaume, M., Murgue, C., Lacroix, B., Therond, O., 2015. The soil-crop models STICS
718 and AqYield predict yield and soil water content for irrigated crops equally well with limited
719 data. Agric. For. Meteorol. 206, 55–68. https://doi.org/10.1016/j.agrformet.2015.02.011
720 Cooper, P.J.M., Dimes, J., Rao, K.P.C., Shapiro, B., Shiferaw, B., Twomlow, S., 2008. Coping better with
721 current climatic variability in the rain-fed farming systems of sub-Saharan Africa: An essential
722 first step in adapting to future climate change? Agric. Ecosyst. Environ. 126, 24–35.
723 https://doi.org/10.1016/j.agee.2008.01.007
724 CORAF/WECARD, 2008. Plan opérationnel 2008-2012. Déployer des systèmes agricoles innovants en
725 Afrique de l'Ouest et du Centre. Dakar, Sénégal, Coraf/Wecard, P10 60.
726 Corre-Hellou, G., Faure, M., Launay, M., Brisson, N., Crozat, Y., 2009. Adaptation of the STICS
727 intercrop model to simulate crop growth and N accumulation in pea–barley intercrops. Field
728 Crops Res. 113, 72–81. https://doi.org/10.1016/j.fcr.2009.04.007
729 Diedhiou, A., Bichet, A., Wartenburger, R., Seneviratne, S.I., Rowell, D.P., Sylla, M.B., Diallo, I., Todzo,
730 S., Touré, N.E., Camara, M., Ngatchah, B.N., Kane, N.A., Tall, L., Affholder, F., 2018. Changes
731 in climate extremes over West and Central Africa at 1.5 °C and 2 °C global warming. Environ.
732 Res. Lett. 13, 065020. https://doi.org/10.1088/1748-9326/aac3e5
733 Falconnier, G.N., Corbeels, M., Boote, K.J., Affholder, F., Adam, M., MacCarthy, D.S., Ruane, A.C.,
734 Nendel, C., Whitbread, A.M., Justes, E., Ahuja, L.R., Akinseye, F.M., Alou, I.N., Amouzou, K.A.,
735 Anapalli, S.S., Baron, C., Basso, B., Baudron, F., Bertuzzi, P., Challinor, A.J., Chen, Y., Deryng,
736 D., Elsayed, M.L., Faye, B., Gaiser, T., Galdos, M., Gayler, S., Gerardeaux, E., Giner, M., Grant,
737 B., Hoogenboom, G., Ibrahim, E.S., Kamali, B., Kersebaum, K.C., Kim, S.-H., van der Laan, M.,
738 Leroux, L., Lizaso, J.I., Maestrini, B., Meier, E.A., Mequanint, F., Ndoli, A., Porter, C.H.,
739 Priesack, E., Ripoche, D., Sida, T.S., Singh, U., Smith, W.N., Srivastava, A., Sinha, S., Tao, F.,
740 Thorburn, P.J., Timlin, D., Traore, B., Twine, T., Webber, H., 2020. Modelling climate change
741 impacts on maize yields under low nitrogen input conditions in sub-Saharan Africa. Glob.
742 Change Biol. 26, 5942–5964. https://doi.org/10.1111/gcb.15261
743 Falconnier, G.N., Journet, E.-P., Bedoussac, L., Vermue, A., Chlébowski, F., Beaudoin, N., Justes, E.,
744 2019. Calibration and evaluation of the STICS soil-crop model for faba bean to explain
745 variability in yield and N2 fixation. Eur. J. Agron. 104, 63–77.
746 https://doi.org/10.1016/j.eja.2019.01.001
747 Gbakatchetche, H., Sanogo, S., Camara, M., Bouet, A., 2010. Effet du paillage par des résidus de pois
748 d'angole (cajanus cajan l.) sur le rendement du riz (oryza sativa) pluvial en zone forestière de
749 CÔTE D'IVOIREE. Agron. Afr. 131–137.
750 Gowing, J.W., Palmer, M., 2008. Sustainable agricultural development in sub-Saharan Africa: the case
751 for a paradigm shift in land husbandry. Soil Use Manag. 24, 92–99.
752 https://doi.org/10.1111/j.1475-2743.2007.00137.x
753 Jayne, T.S., Mason, N.M., Burke, W.J., Ariga, J., 2018. Review: Taking stock of Africa's second-
754 generation agricultural input subsidy programs. Food Policy 75, 1–14.
755 https://doi.org/10.1016/j.foodpol.2018.01.003
756 Knörzer, H., Grözinger, H., Graeff-Hönninger, S., Hartung, K., Piepho, H.-P., Claupein, W., 2011.
757 Integrating a simple shading algorithm into CERES-wheat and CERES-maize with particular
758 regard to a changing microclimate within a relay-intercropping system. Field Crops Res. 121,
759 274–285. https://doi.org/10.1016/j.fcr.2010.12.016
760 Li, L., Yang, S., Li, X., Zhang, F., Christie, P., 1999. Interspecific complementary and competitive
761 interactions between intercropped maize and faba bean. Plant Soil 105–114.
762 Li, L., Zhang, F., Li, X., Christie, P., Sun, J., Yang, S., Tang, C., 2003. Interspecific facilitation of nutrient
763 uptake by intercropped maize and faba bean. Nutr. Cycl. Agroecosystems 61–71.
764 Lidon, B., Francis, F., 1983. Valorisation agricole des ressources pluviométriques : synthèse de
765 l'atelier IRAT-CIEH tenu à Ouagadougou (Burkina) du 27/11 au 4/12/1982. Montpellier :
766 GERDAT-IRAT, 180 p.

Makowski, D., Naud, C., Jeuffroy, M.-H., Barbottin, A., Monod, H., 2006. Global sensitivity analysis for calculating the contribution of genetic parameters to the variance of crop model prediction. Reliab. Eng. Syst. Saf. 91, 1142–1147. https://doi.org/10.1016/j.ress.2005.11.015

Masvaya, E.N., 2019. Risk and crop production intensification options for semi-arid southern Zimbabwe (Thesis). Wageningen University. https://doi.org/10.18174/471607

Pouya, M.B., Bonzi, M., Gnankambary, Z., Traoré, K., Ouédraogo, J.S., Somé, A.N., Sédogo, M.P., 2013. Current soil fertility management practices and their effects on the cotton production and soil on the cotton farms of Central and Western Burkina Faso. Cah. Agric. 22, 282–292. https://doi.org/10.1684/agr.2013.0643

Rezig, M., Sahli, A., Jeddi, F.B., Harbaoui, Y., 2010. Adopting intercropping system for potatoes as practice on drought mitigation under Tunisian conditions. Options Méditerranéennes 329–334.

Ripoche, A., Crétenet, M., Corbeels, M., Affholder, F., Naudin, K., Sissoko, F., Douzet, J.-M., Tittonell, P., 2015. Cotton as an entry point for soil fertility maintenance and food crop productivity in savannah agroecosystems–Evidence from a long-term experiment in southern Mali. Field Crops Res. 177, 37–48. https://doi.org/10.1016/j.fcr.2015.02.013

Sinclair, T.R., Horie, T., 1989. Leaf Nitrogen, Photosynthesis, and Crop Radiation Use Efficiency: A Review. Crop Sci. 29, 90–98. https://doi.org/10.2135/cropsci1989.0011183X002900010023x

Sprent, J.I., Stephens, J.H., Rupela, O.P., 1988. Environmental effects on nitrogen fixation, in: Summerfield, R.J. (Ed.), World Crops: Cool Season Food Legumes, Current Plant Science and Biotechnology in Agriculture. Springer Netherlands, Dordrecht, pp. 801–810. https://doi.org/10.1007/978-94-009-2764-3_64

Stern, R.D., Cooper, P.J.M., 2011. ASSESSING CLIMATE RISK AND CLIMATE CHANGE USING RAINFALL DATA – A CASE STUDY FROM ZAMBIA. Exp. Agric. 47, 241–266. https://doi.org/10.1017/S0014479711000081

Stern, R.D., Dennett, M.D., Garbutt, D.J., 1981. The start of the rains in West Africa. J. Climatol. 1, 59–68. https://doi.org/10.1002/joc.3370010107

Sultan, B., Gaetani, M., 2016. Agriculture in West Africa in the Twenty-First Century: Climate Change and Impacts Scenarios, and Potential for Adaptation. Front. Plant Sci. 7, 20. https://doi.org/10.3389/fpls.2016.01262

Sultan, B., Guan, K., Kouressy, M., Biasutti, M., Piani, C., Hammer, G.L., McLean, G., Lobell, D.B., 2014. Robust features of future climate change impacts on sorghum yields in West Africa. Environ. Res. Lett. 9, 104006. https://doi.org/10.1088/1748-9326/9/10/104006

Tittonell, P., Giller, K.E., 2013. When yield gaps are poverty traps: The paradigm of ecological intensification in African smallholder agriculture. Field Crops Res. 143, 76–90. https://doi.org/10.1016/j.fcr.2012.10.007

Tovignan, T.K., Fonceka, D., Ndoye, I., Cisse, N., Luquet, D., 2016. The sowing date and post-flowering water status affect the sugar and grain production of photoperiodic, sweet sorghum through the regulation of sink size and leaf area dynamics. Field Crops Res. 192, 67–77. https://doi.org/10.1016/j.fcr.2016.04.015

Traore, A., 2015. Analyse de l'évolution à long terme de l'écart de rendement du sorgho dans une rotation coton-sorgho-arachide plus ou moins intensifiée Approche par modélisation (Mémoire de Master). SUPAGRO Montpellier, Montpellier France.

Traore, B., Corbeels, M., van Wijk, M.T., Rufino, M.C., Giller, K.E., 2013. Effects of climate variability and climate change on crop production in southern Mali. Eur. J. Agron. 49, 115–125. https://doi.org/10.1016/j.eja.2013.04.004

Tsubo, M., Mukhala, E., Ogindo, H., Walker, S., 2004. Productivity of maize-bean intercropping in a semi-arid region of South Africa. Water SA 29, 381–388. https://doi.org/10.4314/wsa.v29i4.5038

Vandermeer, J., 1989. The ecology of intercropping, Cambridge University Press. ed. Cambridge.

Vanlauwe, B., Coyne, D., Gockowski, J., Hauser, S., Huising, J., Masso, C., Nziguheba, G., Schut, M., Van Asten, P., 2014. Sustainable intensification and the African smallholder farmer. Curr. Opin. Environ. Sustain. 8, 15–22. https://doi.org/10.1016/j.cosust.2014.06.001

Weih, M., Karley, A.J., Newton, A.C., Kiær, L.P., Scherber, C., Rubiales, D., Adam, E., Ajal, J., Brandmeier, J., Pappagallo, S., Villegas-Fernández, A., Reckling, M., Tavoletti, S., 2021. Grain Yield Stability of Cereal-Legume Intercrops Is Greater Than Sole Crops in More Productive Conditions. Agriculture 11, 255. https://doi.org/10.3390/agriculture11030255

Willey, R.W., 1979. Intercropping-its importance and research needs. Part 1. Competition and yield advantages. Field Crops Abstr 32, 1–10.

Willey, R.W., Rao, M.R., 1980. A Competitive Ratio for Quantifying Competition Between Intercrops. Exp. Agric. 16, 117–125. https://doi.org/10.1017/S0014479700010802

Yang, C., Huang, G., Chai, Q., Luo, Z., 2011. Water use and yield of wheat/maize intercropping under alternate irrigation in the oasis field of northwest China. Field Crops Res. 124, 426–432. https://doi.org/10.1016/j.fcr.2011.07.013

Yu, Y., Stomph, T.-J., Makowski, D., van der Werf, W., 2015. Temporal niche differentiation increases the land equivalent ratio of annual intercrops: A meta-analysis. Field Crops Res. 184, 133–144. https://doi.org/10.1016/j.fcr.2015.09.010

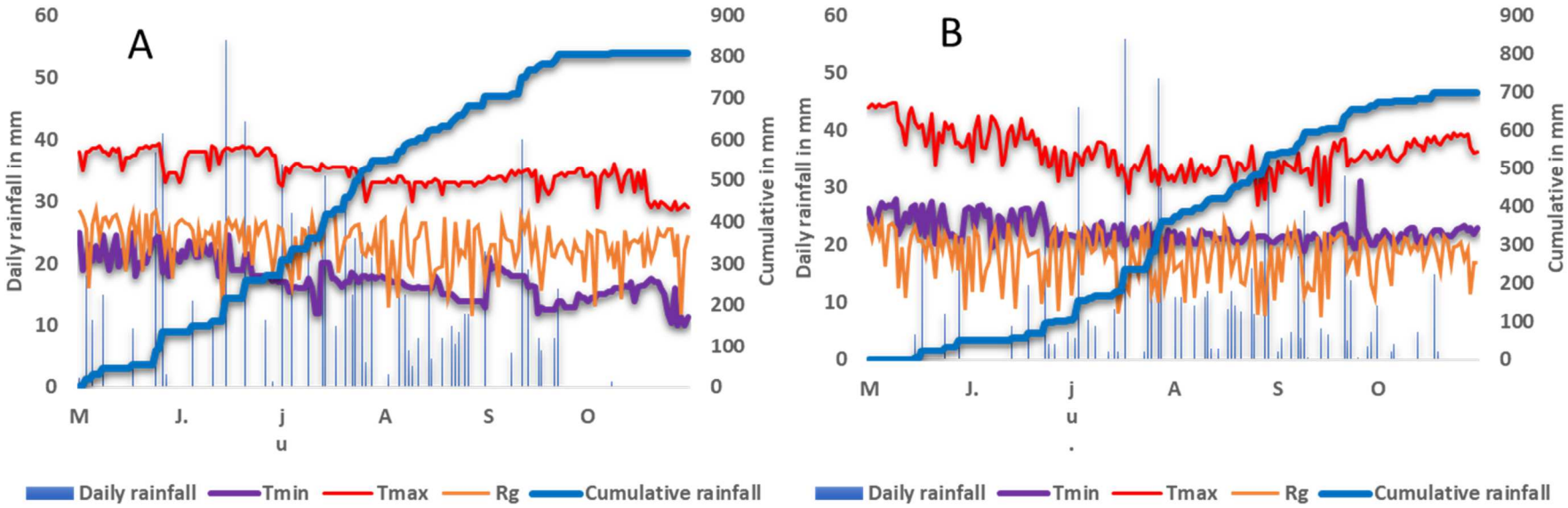

Figure 1: Daily and cumulative rainfall, daily temperature and daily global radiation (Rg) for 2017 (A) and 2018 (B) at the N'Tarla agricultural research station, southern Mali

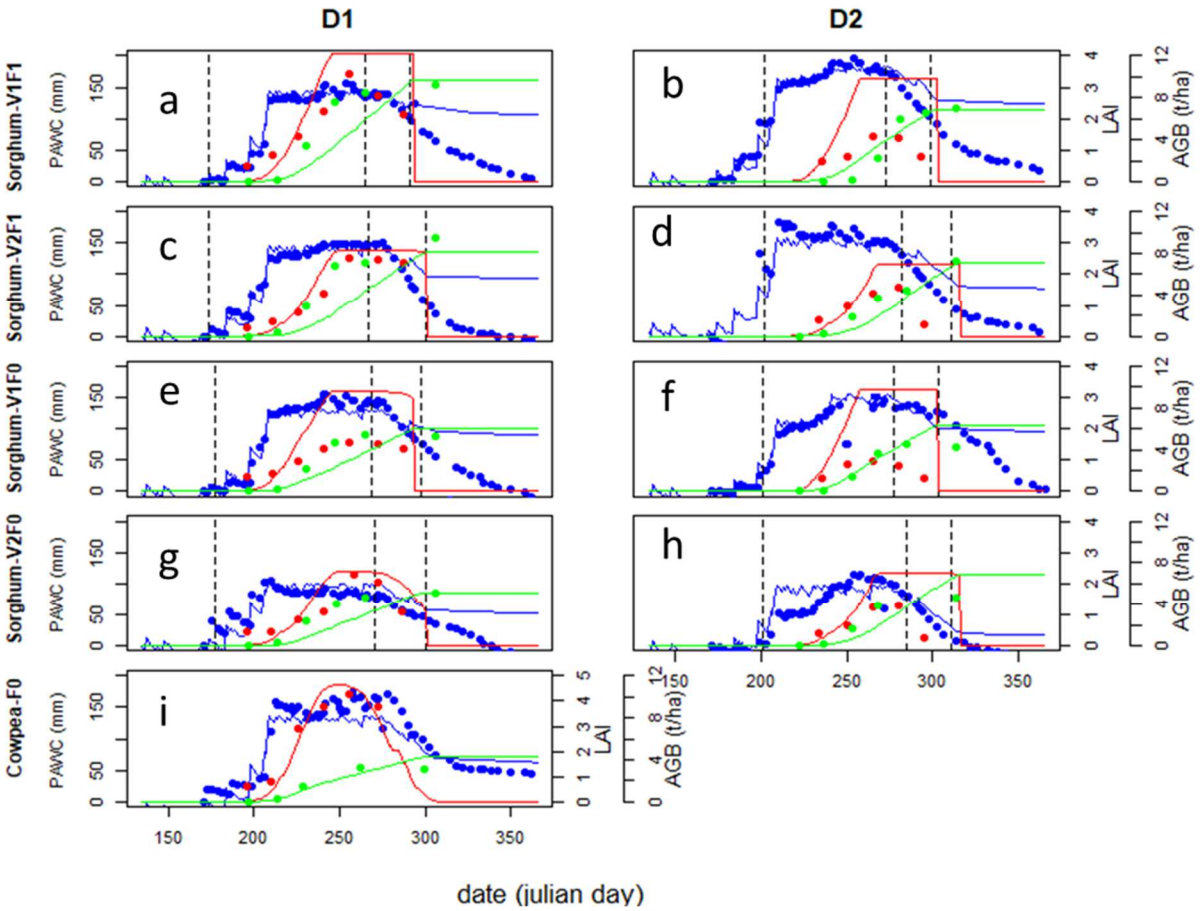

Fig. 2: Observed plant available soil water to maximum measurement depth (PAWC) (blue dots), LAI (red dots), and aboveground biomass (green dots) for the eight sole sorghum simulation units and one sole cowpea simulation unit used for model calibration. The lines are model simulations: blue for soil, red for LAI and green for AGB. Local variety (V1), improved variety (V2), early sowing (D1), late sowing (D2), no fertilizer (F0), 38 kgN ha-1 (F1) at Ntarla research station in 2018. Vertical dotted bars indicate from left to right sowing date, beginning of grain filling and physiological maturity.

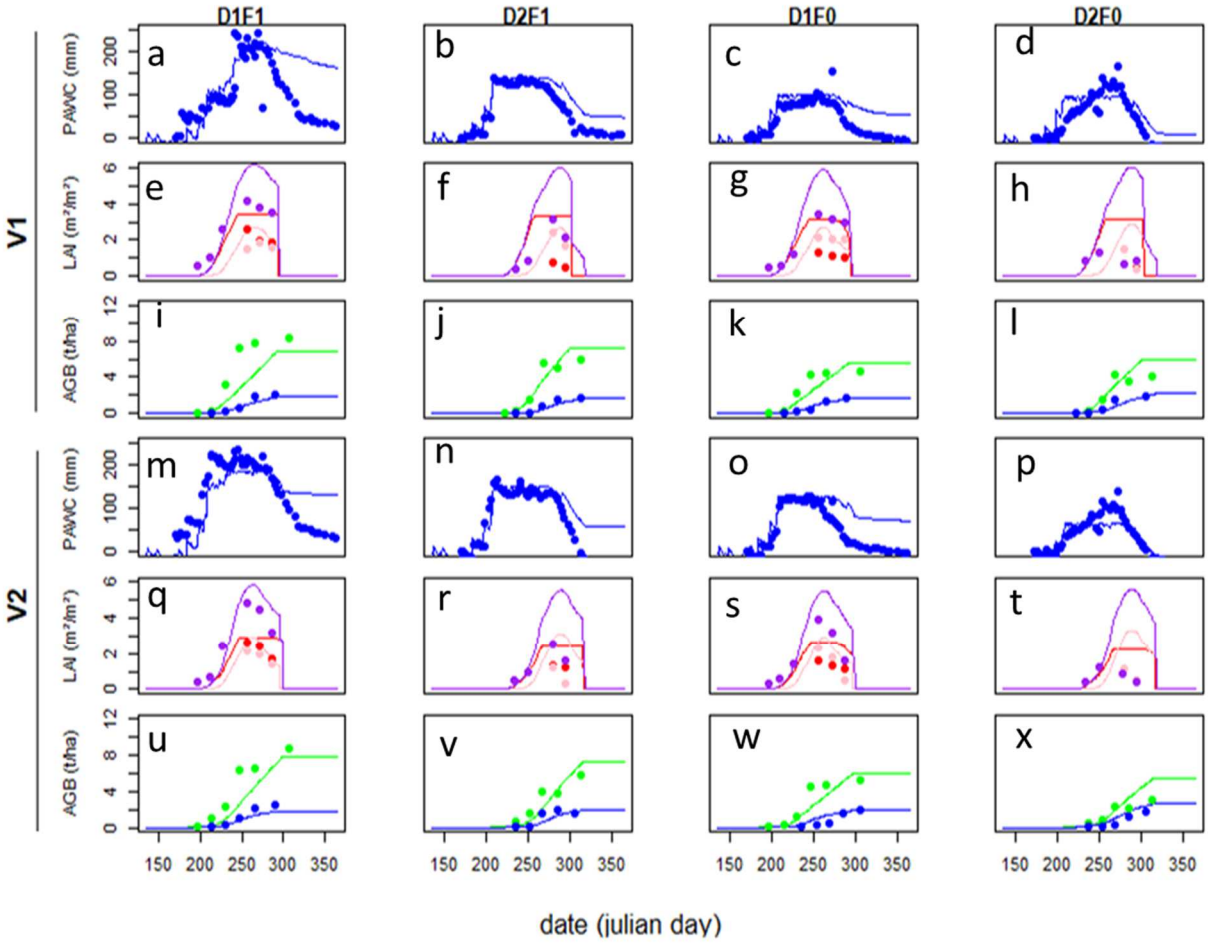

Fig. 3:Observation (blue dots) and simulation (blue line) of plant available soil water to maximum measurement depth (PAWC)(, Fig. a, b, c, d, m n, o, p); observation (purple dots for for sorghum + cowpea, red dots for sorghum in intercropping, pink and transparent dots for cowpea in intercropping) and simulations (lines) of LAI (Fig. e, f, g, h, q, r, s, t,); observation (green dots for sorghum, blue dots for cowpea) and simulations (green lines for sorghum and blue lines for cowpea) of aboveground biomass of sorghum intercropped with cowpea (Fig. i, j, k, l, u, v, w, x). Local variety (V1), improved variety (V2), early sowing (D1), late sowing (D2), 38 kgN ha^{-1} (F1), 0kgNha^{-1} (F0) at Ntarla research station in 2018.

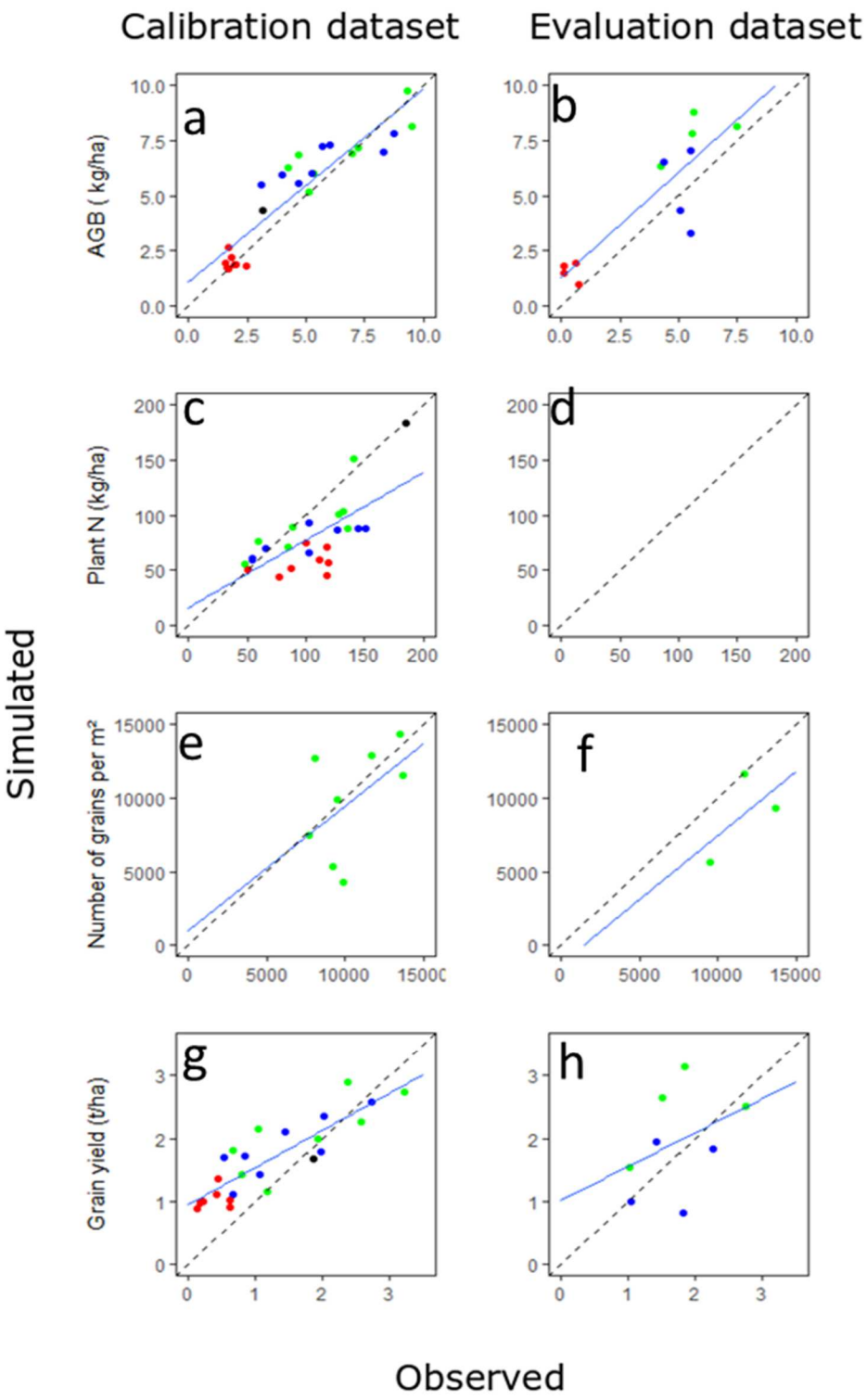

Fig. 4: Observed and STICS simulated aboveground biomass at harvest (AGB), aboveground plant N at harvest (Plant N), number of grains per m² of sorghum at harvest and grain yield for calibration and evaluation datasets (see Table1). There were no observation for cowpea grain yield in 2017 and sorghum and cowpea plant N in the evaluation dataset. The dotted black line is the 1:1 line. The blue line is the regression of simulated values against observed values. Red dots are intercropped cowpea, black dots are sole cowpea, green dots are sole sorghum, blue dots are intercropped sorghum.

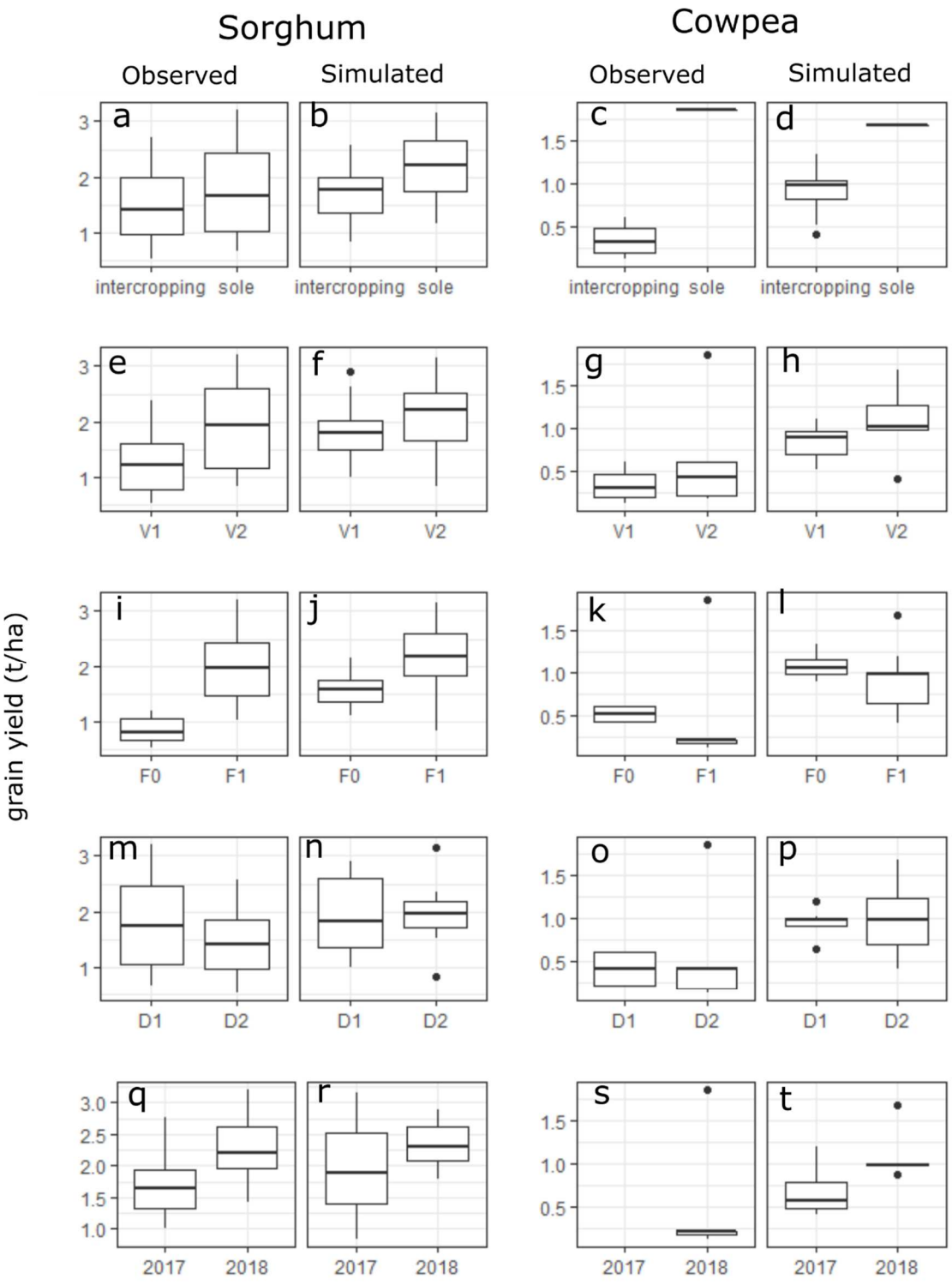

Figure 5: Boxplots of the effect of intercropping, sorghum variety (V1: local, V2: improved), N input (F0 = 0 kgN/ha^{-1}, F1 = 8 kg N/ha^{-1} in 2017 and 38 kgN/ha^{-1} in 2018) and sowing date (D1: early, D2: late) on observed and simulated grain yield. Calibration and evaluation datasets were pooled together. In 2017, there was no sole cowpea plot and no data for cowpea grain yield.

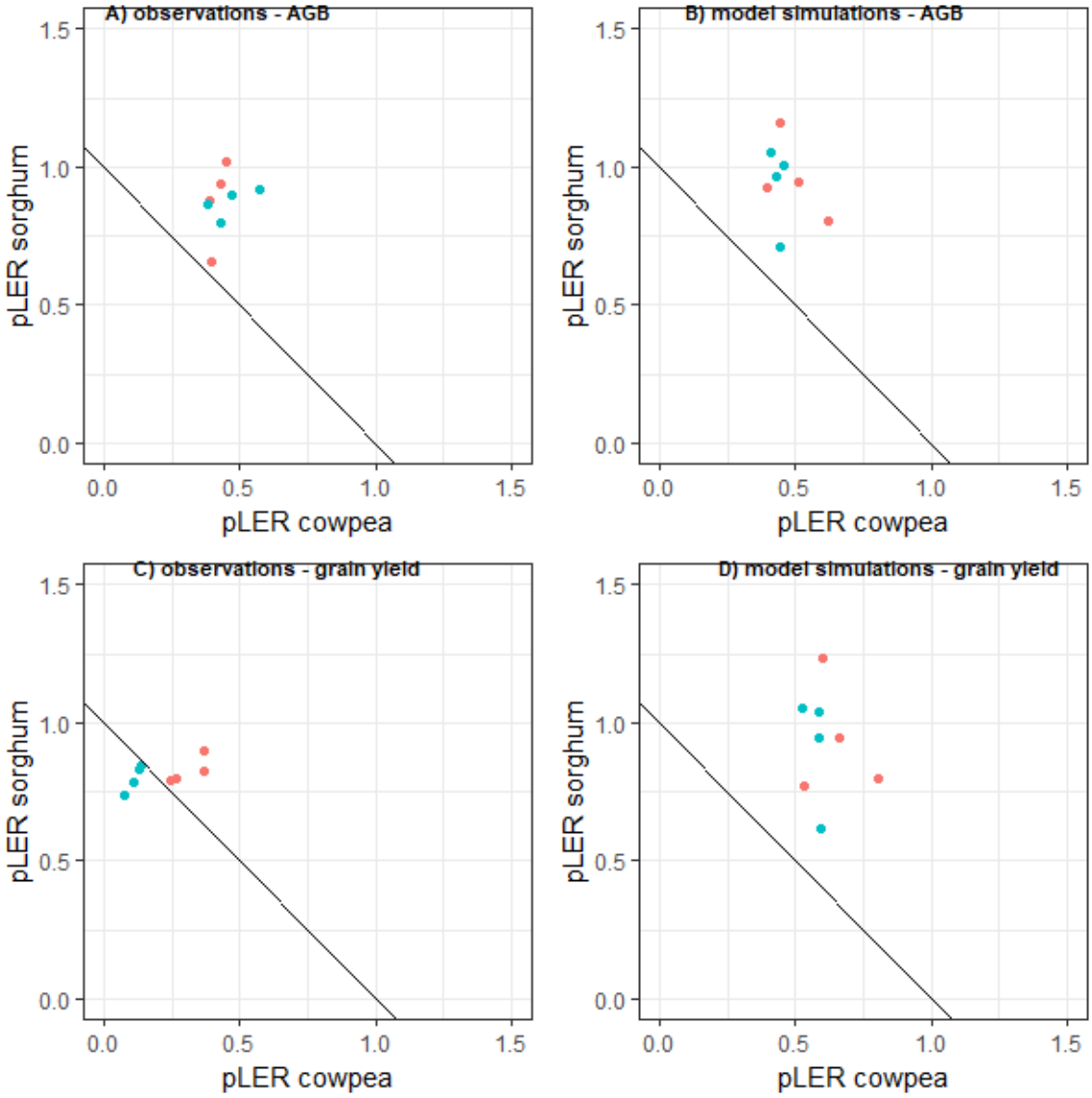

Figure 6: Cowpea and sorghum pLER as observed in the experiment (A for aboveground biomass and C for grain yield) and as simulated by the model (B for aboveground biomass and D for grain yield). Blued dots are F1 (38 kgN ha^{-1}) treatments, and red dots are F0 (0 kgN ha^{-1}) treatments. The black line indicates a LER of 1. Only 2018 experimental plots and simulation units were considered, as in 2017 pLER of cowpea could not be computed because there was no experimental plot with sole cowpea.

Table 1: Description of the experimental plots at the Agronomic Research Station of N'Tarla used for model calibration and evaluation. V1 = Photoperiod-sensitive local sorghum variety, V2 = Improved sorghum variety less sensitive to the photoperiod, D1 = early sowing, D2 = late sowing, F1 = 38 kg N/ha in 2018 and f=8 kg N/ha in 2017, F0 = 0 kg N/ha. Soil water was not measured in 2017.

Dataset	*Year*	Cropping system	Variety	Sowing date	Fertilizer application	Maximum depth of soil water measurement (cm)	Soil organic nitrogen content in the upper layer in %	Name of simulation unit	Field capacity (%).				
									0 - 15 cm	15 – 35 cm	35-55 cm	55-85 cm	85-maximum depth
Calibration	2018	Sole sorghum	V1	D1	F0	115	0.01	V1D1F0	13.7	19	19	19	19
					F1	145	0.02	V1D1F1	13.7	19	19	19	19
				D2	F0	155	0.01	V1D2F0	13.5	19	24	24	24
					F1	155	0.008	V1D2F1	22	25	25	28	19
			V2	D1	F0	95	0.007	V2D1F0	13.7	19	19	18	18
					F1	155	0.011	V2D1F1	13.7	19	19	19	19
				D2	F0	155	0.016	V2D2F0	13.7	19	19	19	22
					F1	155	0.018	V2D2F1	13.7	19	21	21	21
		Sorghum intercropped with cowpea	V1	D1	F0	145	0.015	V1D1F0-inter	13.7	17	17	17	19
					F1	155	0.015	V1D1F1-inter	13.7	23	23	23	23
				D2	F0	155	0.011	V1D2F0-inter	13.7	19	18	18	18
					F1	135	0.011	V1D2F1-inter	13.7	19	19	19	20
			V2	D1	F0	145	0.011	V2D1F0-inter	13.7	17	17	17	17
					F1	155	0.013	V2D1F1-inter	13.7	22	22	22	22
				D2	F0	135	0.012	V2D2F0-inter	13.7	20	20	20	20
					F1	145	0.012	V2D2F1-inter	13.7	22	22	22	22
		Sole Cowpea	Sangaraka	D1	F0	135	0.01	Niebpur	13.7	19	21	21	21**
Evaluation	2017	Sole sorghum	V1	D1	f	-	0.02*	NT17V1D1	13.7	19	19	19	19**
				D2	f	-	0.007*	NT17V1D2	22	25	25	28	19**
			V2	D1	f	-	0.011*	NT17V2D1	13.7	19	19	19	19**
				D2	f	-	0.018*	NT17V2D2	13.7	19	21	21	21**
		Sorghum intercropped with cowpea	V1	D1	f	-	0.015*	NT17V1D1-inter	13.7	23	23	23	23**
				D2	f	-	0.011*	NT17SV1D2-inter	13.7	19	19	19	20**
			V2	D1	f	-	0.013*	NT17V2D1-inter	13.7	19	19	19	20**
				D2	f	-	0.012*	NT17V2D2-inter	13.7	22	22	22	22**

* Not measured in 2017, the values measured in 2018 in the experimental plot were considered. ** maximum depth of soil water measurement for 2018 was considered

Table 2: Description of the crop development stages included in the model

Development stage	Step acronym used in model	Description
Vegetative stages	ILEV	Emergence
	AMF	Maximum acceleration of leaf growth, end of juvenile phase
	ILAX	Maximum leaf area index (LAI), end of leaf growth
Reproductive stages	Flo	Flowering
	IDRP	Start of grain filling
	IMAT	Physiological maturity

Table 3: Values of sorghum parameter as calibrated in the STICS crop model for experiments at N'Tarla in Mali

Parameter				Value			
Process	**acronym**	**Description**	**Target variable**	**V1**	**V2**	**Cowpea**	**Source**
Emergence	tdmin	basal temperature for crop development		8	8	6.2	(Folliard et al. 2004) ; Fao., 2012 ; (Luo 2011).
Crop development	sensiphot	index of photoperiod sensitivity (1=insensitive)		0.4	0.6	-	Trial and error calibration
	phobase	basal photoperiod controlling photoperiod slowing effect		14	14	-	Traroré A., 2015
	phosat	saturating photoperiod controlling photoperiod slowing effect		12,75	12.75	-	Traoré, A., 2015
	stlevamf	cumulative thermal time between emergence and end of juvenile phase	Leaf area index	180	718	881	Test of a range of values
	stamflax	cumulative thermal time between end of juvenile phase and maximum LAI		305	314	687	Trial and error calibration
	stlevdrp	cumulative thermal time between emergence and beginning of grain filling		685	1077	1609	Trial and error calibration
Leaves	dlaimaxbrut	maximum rate of the setting up of LAI		0,0015200	0.01	0.0035	Trial and error calibration
	durvieF	maximal lifespan of an adult leaf		480	280	240	Trial and error calibration
Shoot growth	efcroijuv	maximum radiation use efficiency during the juvenile phase	Aboveground biomass	2.1836	2.1877	1.2	Trial and error calibration
	efcroirepro	maximum radiation use efficiency during the grain filling phase	Aboveground biomass	3.8572	2.8372	1.3559	Trial and error calibration
	efcroiveg	maximum radiation use efficiency during the vegetative stage	Aboveground biomass	3.8049	2.8414	1.7465	Trial and error calibration
	temin	basal temperature for photosynthesis	-	11	11	7.2	(Folliard et al. 2004) ; Fao., 2012 ; (Luo 2011)
	teopt	optimal temperature for photosynthesis	-	25	25	27	(Folliard et al. 2004) ; Fao., 2012 ; (Luo 2011)
	temax	maximal temperature for photosynthesis	-	45	45	40	(Folliard et al. 2004) ; Fao., 2012 ; (Luo 2011)
Nitrogen fixation	fixmaxgr	maximal N symbiotic fixation rate per unit of grain growth rate	N_2 fixed*	-	-	9.5	Trial and error calibration
	fixmaxveg	maximal N symbiotic fixation rate per unit of vegetative growth rate	N_2 fixed*	-	-	30	Trial and error calibration
Nitrogen uptake	Kmabs2	affinity constant of N uptake by roots for the low uptake system	N uptake	40000	37672.32	25000	numerical optimization
	Vmax2	maximum specific N uptake rate with the high affinity transport system	N Uptake	0.1	0.00878	0.06	numerical optimization
Yield formation	cgrain	slope of the relationship between grain number and growth rate	Number of grains	0.06	0.07	0.084	Trial and error calibration
	nbjgrain	Duration in days of the period during which the number of grains can be reduced by stresses	Number of grains	15	15	15	Traoré, A., 2015
	cgrainv0	number of grains produced during the nbjgrains before beginning of grain filling	Number of grains	0	0	0.069	Trial and error calibration
Yield formation	vitircarbe	rate of increase of the C harvest index vs time	grain yield	0.009	0.015	0.01462	Trial and error calibration
	nbgrmax	maximum number of grains	grain yield	25000	60000	1200	Measurement
	pgrainmaxi	maximum weight of one grain	grain yield	0.027	0.0247	0.25	Measurement
	Irmax	maximum harvest index	grain yield	0.3	0.51	0.42	Measurement

*N_2 fixed by the legume was not measured, but estimated for sole cowpea as the difference between the N uptake of sole sorghum without fertilizer and N uptake of sole cowpea.

Table 4: Root mean square error (RMSE), relative root means square error (rRMSE), and efficiency (EF) of STICS simulation of plant variables in the N'Tarla experiment in 2017 and 2018. See Table 1 for details on the calibration and evaluation datasets.

		EF (-)		nRMSE (%)	
Crops	Variable	Calibration	Evaluation	Calibration	Evaluation
Sorghum and cowpea	AGB	0.81	0.58	23	43
	Plant N	-0.05		35	
	Number of grains per m²	-0.28	-2.17	29	25
	Grain yield	0.56	-0.56	49	41
Sorghum only	AGB	0.54	-0.66	21	85
	Plant N	0.26	-	30	-
	Number of grains per m²	-0.28	-2.17	29	25
	Grain yield	0.38	-0.56	41	41
Cowpea only	AGB	-0.09	-0.33	25	99
	Plant N	-0.64	-	42	-
	Number of grains per m²	-	-	-	-
	Grain yield	0.20	-4.66	87	66